Viewing Angle Constraints on S190425z and S190426c and the Joint Gravitational-wave/Gamma-Ray Detection Fractions for Binary Neutron Star Mergers

Hao-Ran Song[1], Shun-Ke Ai[1], Min-Hao Wang[1], Nan Xing[1], He Gao[1] , and Bing Zhang[2]
[1] Department of Astronomy, Beijing Normal University, Beijing 100875, People's Republic of China; gaohe@bnu.edu.cn
[2] Department of Physics and Astronomy, University of Nevada Las Vegas, NV 89154, USA
Received 2019 July 10; revised 2019 August 4; accepted 2019 August 7; published 2019 August 21

Abstract

The Laser Interferometer Gravitational-Wave Observatory (LIGO) and Virgo scientific collaboration (LVC) detected two binary neutron star (BNS) merger candidates, S190425z and S190426c. The *Fermi*-Gamma-ray Burst Monitor (GBM) observed 55.6% (for S190425z) and 100% (for S190426c) of the probability regions of both events at the respective merger times, but no gamma-ray burst (GRB) was detected in either case. The derived luminosity upper limits suggest that a short GRB similar to GRB 170817A would not be detectable for both cases due to their distances, which are larger than that of GW170817. Assuming that the jet profile obtained from GW170817/GRB 170817A is quasi-universal for all BNS–GRB associations, we derive that the viewing angles of S190425z and S190426c should be $>$(0.11–0.41) and $>$(0.09–0.39), respectively. Through Monte Carlo simulations, we show that with the GRB 170817A-like jet structure, all sky gamma-ray detectors, such as GBM and the Gravitational wave high-energy Electromagnetic Counterpart All-sky Monitor, are expected to detect $\sim$4.6%, 3.9%, 1.7%, and 6.6%, 5.7%, 2.8% of BNS mergers triggered by advanced LIGO, A+, and the Einstein Telescope, respectively. The joint detection fraction would be largely reduced for *Swift*-BAT, SVOM-ECLAIRS, and the Einstein Probe, whose sensitivities are better but whose FOVs are smaller.

Unified Astronomy Thesaurus concepts: Gamma-ray bursts (629); Gravitational wave astronomy (675)

1. Introduction

After the exciting discovery of the first binary neutron star (BNS) merger event GW170817 (Abbott et al. 2017a), its associated gamma-ray burst (GRB) 170817A, kilonova, and multi-wavelength afterglows (Abbott et al. 2017b), the Laser Interferometer Gravitational-Wave Observatory (LIGO)-Virgo scientific collaboration (LVC) has recently reported two more candidates that may have BNS merger origins: LIGO/Virgo S190425z and LIGO/Virgo S190426c (The LIGO and the Virgo Collaboration 2019a, 2019b).

S190425z was identified during the real-time processing of data from LIGO Livingston Observatory (L1) and the Virgo Observatory (V1) at 2019 April 25 08:18:05.017 UTC (The LIGO and the Virgo Collaboration 2019a). The false alarm rate is estimated by the online analysis to be 4.5×10^{-13} Hz, or about one in 70 thousands of years. Because the source was not detected by LIGO Hanford (H1) and the signal-to-noise ratio (S/N) was below the threshold in V1, LVC provides a very poor localization constraint. Assuming that the candidate is astrophysical in origin, the probability of classifying this gravitational-wave (GW) event as a BNS merger is greater than 99%. Detailed data analysis is ongoing. Multi-band observations from radio to gamma-rays were immediately undertaken to search for its electromagnetic (EM) counterpart candidate, but no confident counterpart was identified. The Gamma-ray Burst Monitor (GBM) on board the *Fermi* Gamma-Ray Observatory (*Fermi*-GBM) observed 55.6% of the probability region at the merger event time (Fermi GBM Team 2019a). There was no onboard trigger around the event time, and no counterpart candidate was identified with automated, blind, or coherent searches for a GRB signal (from ±30 s around the merger time). The *Fermi*-GBM Team thus estimated that the intrinsic luminosity upper limit for a S190425z-associated-GRB, if any, was $(0.03–6.2) \times 10^{49}$ erg s^{-1}.

S190426c was identified during the real-time processing of data from LIGO Hanford Observatory (H1), LIGO Livingston Observatory (L1), and Virgo Observatory (V1) at 2019 April 26 15:21:55.337 UTC (The LIGO and the Virgo Collaboration 2019b). The false alarm rate for this event is estimated by the online analysis to be 1.9×10^{-8} Hz, or about one in 1 yr and 7 months. Assuming that the candidate is of astrophysical origin, the probability for classifying this GW event as a BNS merger is 49%. Detailed data analysis is ongoing. Similar to S190425z, multi-band observations were carried out immediately to search for an EM counterpart to S190426c, but no confident counterpart has been identified yet. For S190426c, *Fermi*-GBM was observing 100% of the probability region at the merger event time (Fermi GBM Team 2019b). Again, there was no onboard trigger around the event time, and no counterpart candidate was identified with automated, blind, or coherent searches (from ±30 s around the merger time). The *Fermi*-GBM Team thus estimated the intrinsic luminosity upper limit for a S190426c-associated-GRB, if any, as $(0.09–10.6) \times 10^{49}$ erg s^{-1}.

In this work, we show that the luminosity upper limit in the γ-ray band could lead to interesting constraint on the viewing angles of S190425z and S190426c, provided that S190425z and S190426c are associated with a short GRB, whose jet profile is similar to that of GRB 170817A. Moreover, under the hypothesis that the jet profile obtained from the GW170817/GRB 170817A is quasi-universal for all BNS–GRB associations, we perform Monte Carlo simulations to estimate what fraction of BNS mergers detectable by GW detectors is expected to be simultaneously detected in γ-rays.

2. Constraints on the Viewing Angle for S190425z and S190426c

The abnormally low prompt emission luminosity (Goldstein et al. 2017; Zhang et al. 2018a) and the slow rising of the
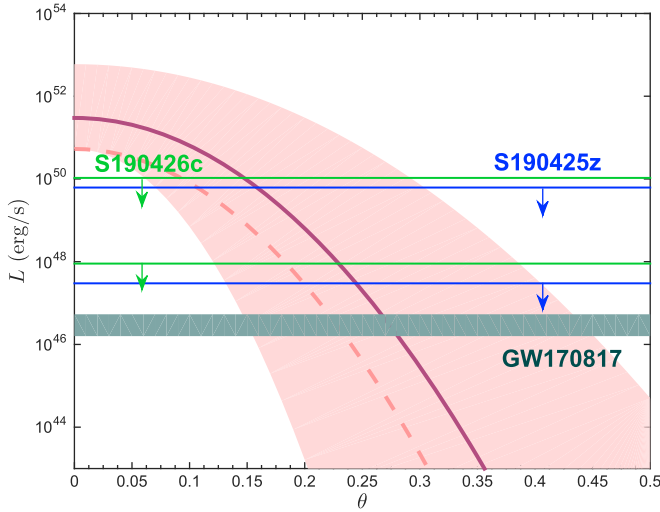
Figure 1. The purple solid line and pink filled region represent the jet profile of GRB 170817A and its 1σ region based on Troja et al. (2018). The dark green region represents the γ-ray emission luminosity of GRB 170817A and the light blue and green solid lines show γ-ray emission luminosity upper limits for S190425z and S190426c. The dashed pink line represents the lower boundary of GRB 170817A jet profile proposed in Finstad et al. (2018).

multi-wavelength light curves (Troja et al. 2017, 2018; Lazzati et al. 2018; Lyman et al. 2018; Mooley et al. 2018) of GRB 170817A suggested that the event is best interpreted as a structured jet (e.g., Rossi et al. 2002; Zhang & Mészáros 2002) with a large viewing angle from the jet axis. With a broadband study and a multi-messenger analysis including the GW constraints, it has been proposed that the data of GW170817/GRB 170817A favor a Gaussian-shaped jet profile (Zhang & Mészáros 2002; Alexander et al. 2018; Lazzati et al. 2018; Mooley et al. 2018; Troja et al. 2018; Ghirlanda et al. 2019)

$$E(\theta) = E_0 \exp\left(-\frac{\theta^2}{2\theta_c^2}\right) \qquad (1)$$

for $\theta \leqslant \theta_w$, where E_0 is the on-axis equivalent isotropic energy, θ_c is the characteristic angle of the core, and θ_w is the truncating angle of the jet. Such a Gaussian jet profile seems to be supported by numerical simulations of a short GRB jet propagates in a dynamical ejecta with a negligible waiting time of jet launching (Xie et al. 2018; Geng et al. 2019). In order to interpret the multi-wavelength EM observations and the viewing angle constraint from the GW analysis, Troja et al. (2018) proposed $\theta_c = 0.057^{+0.025}_{-0.023}$, $\log_{10} E_0 = 52.73^{+1.3}_{-0.75}$ and $\theta_w = 0.62^{+0.65}_{-0.37}$ for the jet profile of GRB 170817A. The value of the Hubble constant reported by the Planck collaboration (Planck Collaboration et al. 2016) was adopted.

In Figure 1, we plot the jet profile of GRB 170817A with the 1σ region as proposed by Troja et al. (2018), the γ-ray emission luminosity of GRB 170817A, and the γ-ray emission luminosity upper limits for S190425z and S190426c. Note that in order to convert the energy profile in Troja et al. (2018) to the luminosity profile, here we assume that the γ-ray radiation efficiency is 10%, the burst duration $T_{90} \sim 2\,\mathrm{s}$ and the spectrum is flat. Such a jet profile covers the regime of known short GRBs, and the hypothesis of a quasi-universal structured jet for all short GRBs seems to be consistent with the currently available data (Beniamini et al. 2019; Salafia et al. 2019). Assuming that both S190425z and

S190426c are associated with a short GRB, whose jet profile is similar to that of GRB 170817A, we derive that the viewing angle of S190426c is >(0.06–0.39), with the uncertainty mainly defined by the uncertainty of its luminosity distance. As shown in Figure 1, the uncertainty of the jet profile considered here is already wide enough to accommodate a variety of possible quasi-universal structures, so our conclusion is generally valid if the jet structure of individual GRBs deviates from the Gaussian form but generally falls into the shaded region in Figure 1. For S190425z, with an additional assumption that its location was within the FOV of *Fermi*-GBM, one can derive its viewing angle as being >(0.07–0.41), with the uncertainty again mainly defined by the uncertainty of its luminosity distance at the merger time. It is worth noticing that Finstad et al. (2018) performed a joint analysis of the GW/EM observations and suggested a conservative lower limit on the viewing angle of >13° for GRB 170817A. If one takes this limit, the lower boundary of GRB 170817A jet profile would become tighter (dashed line in Figure 1), so that the viewing angle constraint for both S190425z and S190426c would become tighter, i.e., >(0.09–0.39) for S190426c and >(0.11–0.41) for S190425z, respectively.

3. γ-Ray Detection Rate for GW Triggers

Assuming that the jet profile obtained from the GW170817/GRB 170817A is quasi-universal for all BNS–GRB associations, here we perform Monte Carlo simulations to estimate what fraction of BNS mergers detectable by GW detectors is expected to be also detected by γ-ray detectors, such as *Fermi*-GBM (Meegan et al. 2009), Neil Gehrels *Swift*-BAT (Gehrels et al. 2004), the future Chinese–French GRB mission SVOM-ECLAIRS (Götz et al. 2014), and the future Chinese mission Gravitational wave high-energy Electromagnetic Counterpart All-sky Monitor (GECAM; Zhang et al. 2018b), and by large field-of-view (FOV) X-ray detectors, such as the future Chinese mission Einstein Probe (EP; Yuan et al. 2018b).

3.1. Sample for BNS Mergers Detectable by GW Detectors

The event-rate density for BNS mergers at a given redshift z could be estimated as

$$N(z) = \frac{R_{\mathrm{NS-NS\,merger,0}} \times f(z)}{1+z} \frac{dV(z)}{dz}, \qquad (2)$$

where $R_{\mathrm{NS-NS\,merger,0}} = 1540^{+3200}_{-1220}\,\mathrm{Gpc}^{-3}\,\mathrm{yr}^{-1}$ is the local NS–NS merger rate (Abbott et al. 2017a), $f(z)$ is the the dimensionless redshift distribution factor, and $dV(z)/dz$ is the differential comoving volume $dV(z)/dz$, which reads

$$\frac{dV(z)}{dz} = 4\pi\left(\frac{c}{H_0}\right)^3\left(\int_0^z \frac{dz}{\sqrt{1-\Omega_m + \Omega_m(1+z)^3}}\right)^2$$
$$\times \frac{1}{\sqrt{1-\Omega_m + \Omega_m(1+z)^3}}. \qquad (3)$$

Here Planck results are adopted for cosmological parameters, e.g., $H_0 = 67.8\,\mathrm{km\,s^{-1}\,Mpc^{-1}}$, $\Omega_m = 0.308$, and $\Omega_\Lambda = 0.692$ (Planck Collaboration et al. 2016).

The function $f(z)$ depends on the initial redshift distribution of BNS systems and the delay time distribution for BNS systems going through the inspiral phase to the merger. We first assume the initial redshift distribution of BNS systems track the star formation rate (SFR) in units of $M_\odot\,\mathrm{Gpc}^{-3}\,\mathrm{yr}^{-1}$, which

could be empirically expressed as (Yuksel et al. 2008)

$$\mathrm{SFR}(z) \propto \left[(1+z)^{3.4\eta} + \left(\frac{1+z}{5000}\right)^{-0.3\eta} + \left(\frac{1+z}{9}\right)^{-3.5\eta}\right]^{\frac{1}{\eta}}.$$

$$(4)$$

Sun et al. (2015) have investigated three main types of delay time distributions (i.e., Gaussian distribution, Virgili et al. 2011; power-law distribution, Mooley et al. 1992; and log-normal distribution, Wanderman & Piran 2015) and suggested that the power-law model leads to a wider redshift distribution of NS–NS merger than other two models, which is disfavored by the short GRB data. In this work, log-normal delay time distribution is assumed as an example, the formula for which reads

$$m(\tau) = \exp\left(-\frac{(\ln\tau - \ln t_d)^2}{2\sigma^2}\right)/(\sqrt{2\pi}\,\sigma),$$

$$(5)$$

with $t_d = 2.9$ Gyr and $\sigma = 0.2$. We randomly generate 10^7 binary NS systems following the redshift distribution described by Equation (2), with redshift ranging from 0 to 3.

For each binary NS system, their NS masses (m_1 and m_2) are generated following the observationally derived distribution of Galactic NS–NS systems; i.e., M_{BNS} has a normal distribution $N(\mu_{\mathrm{BNS}} = 1.32\,M_\odot, \sigma_{\mathrm{BNS}} = 0.11)$, with a mean μ_{BNS} and a standard deviation σ_{BNS} (Kiziltan et al. 2013), and their viewing angles are generated with a uniform distribution in the directional space ($N(\theta) \propto \sin(\theta)$).

Here we estimate the GW signal's amplitude during the inspiral phase within the Newtonian approximation condition as

$$h_+ = -\frac{2G\mu}{c^2 D_L}(1 + \cos^2\theta)\left(\frac{v}{c}\right)^2\cos 2\varphi \quad (6)$$

$$h_\times = -\frac{4G\mu}{c^2 D_L}\cos\theta\left(\frac{v}{c}\right)^2\sin 2\varphi, \quad (7)$$

where $+$ and $\times$ are two polarizations of the GW signal, $\mu = m_1 m_2/(m_1 + m_2)$ is the reduced mass, D_L presents the luminosity distance of the BNS system, θ is the viewing angle, and $v = (\pi GMf)^{1/3}$ is the Equivalent linear velocity ($f = 2f_{\mathrm{orbital}} = \omega/\pi$ is GW signal's frequency). The evolution of v over time is

$$\frac{d(v/c)}{dt} = \frac{32\eta}{5}\frac{c^3}{GM}\left(\frac{v}{c}\right)^9, \quad (8)$$

where $M = m_1 + m_2$ is the total mass and $\eta = (m_1 m_2)/M^2$ is the dimensionless reduced mass.

Given the sensitivity curve of GW detectors, the signal-to-noise ratio (S/N) of GW detection for each BNS mergers could be estimated as (Corsi & Mészáros 2009)

$$\langle S/N \rangle^2 = \int_{f_{\min}}^{f_{\max}} \frac{h_c(f)^2}{fS_n} d\ln f. \quad (9)$$

where S_n is the power spectral density (PSD) of the detector noise, $f_{\min}$ and $f_{\max}$ define the frequency range of the signal from 10 to 2000 Hz, and h_c is a characteristic amplitude in the

frequency domain, which reads

$$h_c = fh(t)\sqrt{\frac{dt}{df}}. \quad (10)$$

where $h(t) = \sqrt{h_+^2 + h_\times^2}$. Here we consider the designed PSD for aLIGO (Abramovici et al. 1992) and aLIGO A+ (LIGO Scientific Collaboration 2016), as well as the proposed third-generation GW detectors (i.e., ET Punturo et al. 2010, CE Abbott et al. 2017c). We set S/N larger than 16 as the criteria for GW triggers in our simulation.

3.2. γ-Ray Flux Distribution and Detection Rate

We assume that every GW-triggered event in our simulation successfully launches a relativistic jet with a quasi-universal jet profile described in Equation (1). For each case, E_0, θ_c, and θ_w are generated following the best-fit distribution inferred from GRB 170817 (Troja et al. 2018), i.e., $\theta_c = 0.057^{+0.025}_{-0.023}$, $\log_{10}E_0 = 52.73^{+1.3}_{-0.75}$ and $\theta_w = 0.62^{+0.65}_{-0.37}$. Given the viewing angle θ, the γ-band flux for each BNS system could be estimated as

$$F_\gamma = \frac{E_0\eta_\gamma}{4\pi D_L^2}\exp\left(-\frac{\theta^2}{2\theta_c^2}\right), \quad (11)$$

where η_γ is the radiative efficiency. Here we adopt $\eta_\gamma = 0.1$ for the bolometric energy flux in the 1–10^4 keV band. Assuming that the gamma-ray spectrum for all simulated BNS-associated-GRBs follow the band function with photon indices -1 and -2.3 (Preece et al. 2000) below and above E_p, respectively, we can estimate the corresponding flux for a specific γ-ray detector with a given observational energy band, and then justify whether or not the simulated source can be detected. Note that the bolometric isotropic luminosity and the peak energy for GRB 170817A does not satisfy the Yonetoku relation (Yonetoku et al. 2004). Within the Gaussian structure jet framework, Ioka & Nakamura (2019) proposed that the profile that E_p changes with the viewing angle θ should be $E_p(\theta) = E_{p,0} \times (1 + \theta/\theta_c)^{-0.4}$, where $E_{p,0}$ and the central luminosity of the Gaussian jet satisfy the Yonetoku relation. Such a prescription allows the GRB 170817A observations to be incorporated with the historical short GRB statistical data. For each simulated GRB, we use such a profile to estimate its E_p value. The accumulative distribution of bolometric F_γ (in the 1–10^4 keV band) for different GW detectors is shown in Figure 2, together with the effective sensitivity limit for various γ-ray detectors. Here the sensitivity for *Fermi*-GBM is adopted as $\sim 2 \times 10^{-7}$ erg s^{-1} in 50–300 keV (Meegan et al. 2009), and the sensitivity for GECAM is adopted as $\sim 1 \times 10^{-7}$ erg s^{-1} in 50–300 keV (Zhang et al. 2018b). For *Swift*-BAT and SVOM-ECLAIRS, we adopt the same sensitivity as $\sim 1.2 \times 10^{-8}$ erg s^{-1} in 15–150 keV (Gehrels et al. 2004; Götz et al. 2014). The sensitivity for EP is adopted as $\sim 3 \times 10^{-9}$ erg s^{-1} in 0.5–4 keV (Yuan et al. 2018a).

We can see that with a GRB 170817A-like jet structure, less than 10% of GW-triggered BNS mergers would have a γ-ray flux that is higher than the threshold of the current (or near-future) γ-ray detectors. For instance, the γ-ray flux of 6.3% of the aLIGO detectable BNS mergers are above the sensitivity limit of *Fermi*-GBM. Considering that the average FOV of *Fermi*-GBM is around three-quarters of the whole sky, $\sim 4.6\%$ of BNS mergers detectable by aLIGO is expected to be simultaneously detected by
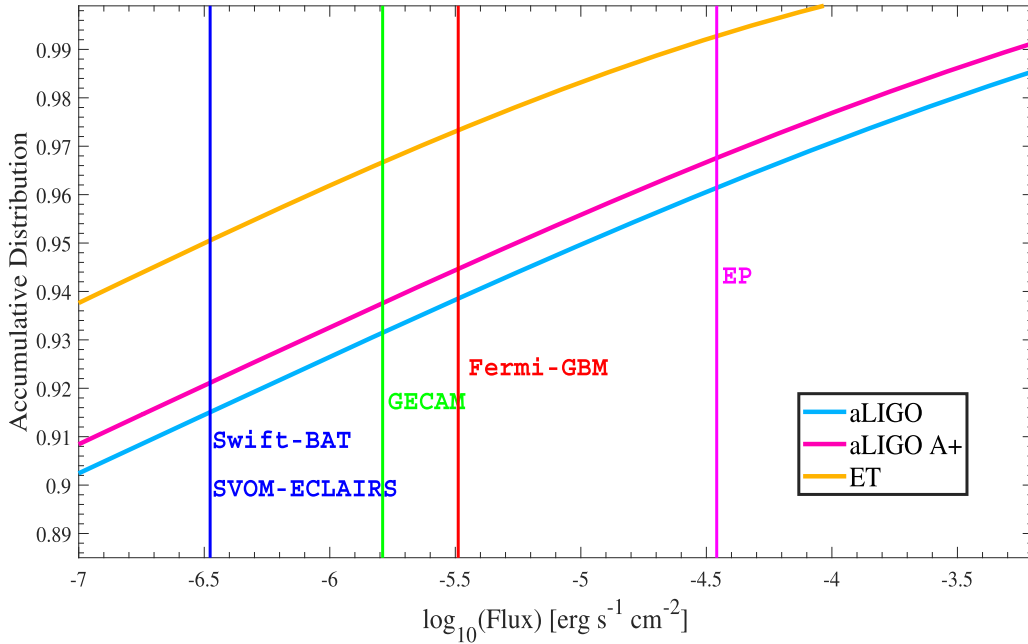
Figure 2. Accumulative distribution of bolometric flux in the $1-10^4$ keV band for BNS mergers triggered by aLIGO, aLIGO A+, and ET. The vertical colored lines show the effective sensitivity of *Fermi*-GBM, *Swift*-BAT, SVOM-ECLAIRS, GECAM, and EP, which correspond to band function spectrum with $\alpha = -1$, $\beta = -2.3$ and E_p equaling to the mean value for the simulated sample.

Table 1
The Joint Detection Rate of Five Gamma-Ray Missions and three GW Detectors

	Fermi-GBM	GECAM	*Swift*-BAT	SVOM-ECLAIRS	EP
aLIGO	4.61% (1.83 yr^{-1})	6.57% (2.61 yr^{-1})	0.977% (0.388 yr^{-1})	1.68% (0.668 yr^{-1})	0.366% (0.145 yr^{-1})
aLIGO A+	3.87% (8.40 yr^{-1})	5.72% (12.4 yr^{-1})	0.887% (1.92 yr^{-1})	1.53% (3.31 yr^{-1})	0.266% (0.578 yr^{-1})
ET	1.69% (593 yr^{-1})	2.83% (990 yr^{-1})	0.536% (188 yr^{-1})	0.924% (324 yr^{-1})	0.112% (39.2 yr^{-1})

Fermi-GBM. As more distant sources become detectable, the fraction for GW-triggered BNSs being simultaneously detected by *Fermi*-GBM would be reduced to ~3.9% and ~1.7% for aLIGO A+ and ET, but the absolute detection rate should largely increase. The proposed sensitivity of GECAM is slightly better than *Fermi*-GBM, and its proposed FOV is around 4π. In this case, we find that ~6.6%, 5.7% and 2.8% of BNS mergers detectable by aLIGO, aLIGO A+, and ET are expected to be simultaneously detected by GECAM, respectively. The sensitivity of *Swift*-BAT and SVOM-ECLAIRS are better than *Fermi*-GBM and GECAM, but their FOVs are much smaller (~one-ninth of the whole sky for Swift and ~one-fifth for SVOM-ECLAIRS; Chu et al. 2016). In this case, we expect ~0.98%, 0.89% and 0.54% of BNS mergers triggered by aLIGO, aLIGO A+, and ET are detectable with *Swift*-BAT, and ~1.7%, 1.5%, and 0.9% of BNS mergers triggered by aLIGO, aLIGO A+, and ET are detectable with SVOM-ECLAIRS. The EP has an FOV that is ~one-eleventh of the whole sky, which results in a small observation rate, ~0.37%, 0.27%, and 0.11%. The joint detection fraction and absolute joint detection rate of five gamma-ray missions and three GW detectors are collected in Table 1.

4. Conclusion and Discussion

Assuming that every BNS merger is associated with a short GRB, whose jet profile is broadly similar to that of GRB 170817A, here we show that even the luminosity upper limit in

the γ-ray band could lead to interesting constraint on the viewing angles of GW-triggered BNS mergers. For instance, we derive that the viewing angles of S190425z and S190426c should be >(0.11–0.41) and >(0.09–0.39), respectively. A 170817A-like short GRB would be undetectable for S190425z and/or S190426c due to their larger distances than GW170817/GRB 170817A. The constraints have to be revised in the following situations. 1.) S190425z and/or S190426c are not from BNS mergers. 2.) S190425z was not in the FOV of GBM (e.g., blocked by Earth). 3.) Not all BNS mergers are associated with short GRBs. 4.) BNS short GRBs do not share a quasi-universal jet structure. If our interpretation is correct, however, the constraints on viewing angle would be helpful for GW data analysis to reach better constraints on the binary properties.

Furthermore, with Monte Carlo simulations we find that with GRB 170817A-like jet structure, all sky gamma-ray detectors, such as GBM and GECAM, are expected to detect 4.6%, 3.9%, 1.7% and 6.6%, 5.7%, 2.8% of BNS mergers triggered by aLIGO, aLIGO A+, and ET, respectively. For *Swift*-BAT, SVOM-ECLAIRS, and EP, whose sensitivities are better but FOVs are smaller, the simultaneous GW/γ-ray detection fraction would be largely reduced. Future joint observations of BNS GW sources by LVC and all sky gamma-ray detectors, such as GBM and GECAM, together with the event-rate density studies (e.g., Sun et al. 2015; Zhang et al. 2018a), will finally test the quasi-universal jet hypothesis of BNS mergers.

In our Monte Carlo simulations, in order to justify whether or not the simulated sources could be detected by the gamma-ray detectors, we simply compare the integrated flux with the effective γ-ray detector sensitivities. In practice, the detection rates for the various detectors depend on the details of the triggering algorithm and sky background for each detector, particularly for the sources near the effective sensitivity limit. Future work is needed to give more precise predictions for specific γ-ray detectors, but we expect that the results should be consistent with the results here to orders of magnitude. Also, in our simulations we take the posterior jet-parameter distributions from one single measurement of GRB 170817A and regard it as the representative of the physical parameter distributions for all BNS-associated-short-GRB populations. The detection rate would be altered if the jet structure of GRB 170817A is not representative. The detection rate would increase if the jet structure for the population is broader than GRB 170817A, and vice versa. More BNS-associated-short-GRB detections in the future will help to better draw the jet structure for the population, which would lead to more precise estimations for the detection rates.

ORCID iDs

He Gao ⦿ https://orcid.org/0000-0002-3100-6558
Bing Zhang ⦿ https://orcid.org/0000-0002-9725-2524

References

Abbott, B. P., Abbott, R., Abbott, T. D., et al. 2017a, PhRvL, 118, 221101
Abbott, B. P., Abbott, R., Abbott, T. D., et al. 2017b, ApJL, 848, L12
Abbott, B. P., Abbott, R., Abbott, T. D., et al. 2017c, CQGra, 34, 044001
Abramovici, A., Althouse, W. E., Drever, R. W. P., et al. 1992, Sci, 256, 325
Alexander, K. D., Margutti, R., Blanchard, P. K., et al. 2018, ApJL, 863, L18
Band, D., Matteson, J., Ford, L., et al. 1993, ApJ, 413, 281
Barthelmy, S. D., Barbier, L. M., Cummings, J. R., et al. 2005, SSRv, 120, 143
Beniamini, P., Petropoulou, M., Barniol Duran, R., et al. 2019, MNRAS, 483, 840
Chu, Q., Howell, E. J., Rowlinson, A., et al. 2016, MNRAS, 459, 121
Corsi, A., & Mészáros, P. 2009, ApJ, 702, 1171
Fermi GBM Team 2019a, GCN, 24185, 1
Fermi GBM Team 2019b, GCN, 24248, 1
Finstad, D., De, S., Brown, D. A., Berger, E., & Biwer, C. M. 2018, ApJL, 860, L2
Gehrels, N., Chincarini, G., Giommi, P., et al. 2004, ApJ, 611, 1005
Geng, J.-J., Zhang, B., Kölligan, A., et al. 2019, ApJL, 877, L40
Ghirlanda, G., Salafia, O. S., Paragi, Z., et al. 2019, Sci, 363, 968
Goldstein, A., Veres, P., Burns, E., et al. 2017, ApJL, 848, 14L
Götz, D., Osborne, J., Cordier, B., et al. 2014, Proc. SPIE, 9144, 914423
Ioka, K., & Nakamura, T. 2019, MNRAS, 487, 4884
Kiziltan, B., Kottas, A., De Yoreo, M., & Thorsett, S. E. 2013, ApJ, 778, 66
Lazzati, D., Perna, R., Morsony, B. J., et al. 2018, PhRvL, 120, 241103
LIGO Scientific Collaboration 2016, The LSC-Virgo White Paper on Instrument Science, LIGO-T1600119-v4, https://dcc.ligo.org/LIGO-T1600119/public
Lyman, J. D., Lamb, G. P., Levan, A. J., et al. 2018, NatAs, 2, 751
Meegan, C., Lichti, G., Bhat, P. N., et al. 2009, ApJ, 702, 791
Mooley, K. P., Nakar, E., Hotokezaka, K., et al. 1992, ApJL, 389, L45
Mooley, K. P., Nakar, E., Hotokezaka, K., et al. 2018, Natur, 554, 207
Planck Collaboration, Ade, P. A. R., Aghanim, N., et al. 2016, A&A, 594, A13
Preece, R. D., Briggs, M. S., Mallozzi, R. S., et al. 2000, ApJS, 126, 19
Punturo, M., Abernathy, M., Acernese, F., et al. 2010, CQGra, 27, 194002
Rossi, E., Lazzati, D., & Rees, M. J. 2002, MNRAS, 332, 945
Salafia, O. S., Ghirlanda, G., Ascenzi, S., et al. 2019, A&A, 628, A18
Sun, H., Zhang, B., & Li, Z. 2015, ApJ, 812, 33
The LIGO and the Virgo Collaboration 2019a, GCN, 24237, 1
The LIGO and the Virgo Collaboration 2019b, GCN, 24168, 1
Troja, E., Piro, L., Ryan, G., et al. 2018, MNRAS, 487, L18
Troja, E., Piro, L., van Eerten, H., et al. 2017, Natur, 551, 71T
Virgili, F. J., Zhang, B., O'Brien, P., & Troja, E. 2011, ApJ, 727, 109
Wanderman, D., & Piran, T. 2015, MNRAS, 448, 3026
Xie, X., Zrake, J., & MacFadyen, A. 2018, ApJ, 863, 58
Yonetoku, D., Murakami, T., Nakamura, T., et al. 2004, ApJ, 609, 935
Yuan, W., Zhang, C., Chen, Y., et al. 2018a, SSPMA, 48, 039502
Yuan, W., Zhang, C., Ling, Z., et al. 2018b, Proc. SPIE, 10699, 1069925
Yuksel, H., Kistler, M. D., Beacom, J. F., et al. 2008, ApJL, 683, L5
Zhang, B., & Mészáros, P. 2002, ApJ, 571, 876
Zhang, B.-B., Zhang, B., Sun, H., et al. 2018a, NatCo, 9, 447
Zhang, D.-L., Li, X.-Q., Xiong, S.-L., et al. 2018b, arXiv:1804.04499